

Review

Nanostructured Photocatalysts and Their Applications in the Photocatalytic Transformation of Lignocellulosic Biomass: An Overview

Juan Carlos Colmenares ^{1,*}, Rafael Luque ^{2,*}, Juan Manuel Campelo ², Fernando Colmenares ^{3,4}, Zbigniew Karpiński ¹ and Antonio Angel Romero ²

¹ Institute of Physical Chemistry, Polish Academy of Sciences, ul. Kasprzaka 44/52, 01-224 Warszawa, Poland; E-Mail: zk@ichf.edu.pl (Z.K.)

² Departamento de Química Orgánica, Universidad de Córdoba, Edificio Marie Curie, Ctra Nnal IV, Km 396, E-14014, Córdoba, Spain; E-Mails: qo1capej@uco.es (J.M.C.); qo1rorea@uco.es (A.A.R.)

³ School of Engineering, Cranfield University, Cranfield, Bedfordshire, MK43 0AL, UK; E-Mail: r.f.colmenaresquintero@Cranfield.ac.uk (F.C.)

⁴ Gas Turbine Engineering Group, Faculty of Engineering, University of St. Bonaventure, Cra. 8H No. 172-20, Bogotá, D.C., Colombia

* Authors to whom correspondence should be addressed; E-Mails: jcarlos@ichf.edu.pl (J.C.C.); q62alsor@uco.es (R.L.); Tel.: +48223433215 (J.C.C.); +34957212065 (R.L.); Fax: +34957212066.

Received: 7 November 2009; in revised form: 27 November 2009 / Accepted: 2 December 2009 /

Published: 7 December 2009

Abstract: Heterogeneous photocatalysis offer many possibilities for finding appropriate environmentally friendly solutions for many of the the problems affecting our society (*i.e.*, energy issues). Researchers are still looking for novel routes to prepare solid photocatalysts able to transform solar into chemical energy more efficiently. In many developing countries, biomass is a major energy source, but currently such countries lack of the technology to sustainably obtain chemicals and/or fuels from it. The Roadmap for Biomass Technologies, authored by 26 leading experts from academia, industry, and government agencies, has predicted a gradual shift back to a carbohydrate-based economy. Biomass and biofuels appear to hold the key to satisfy the basic needs of our societies for the sustainable production of liquid fuels and high value-added chemicals without compromising the scenario of future generations. In this review, we aim to discuss various

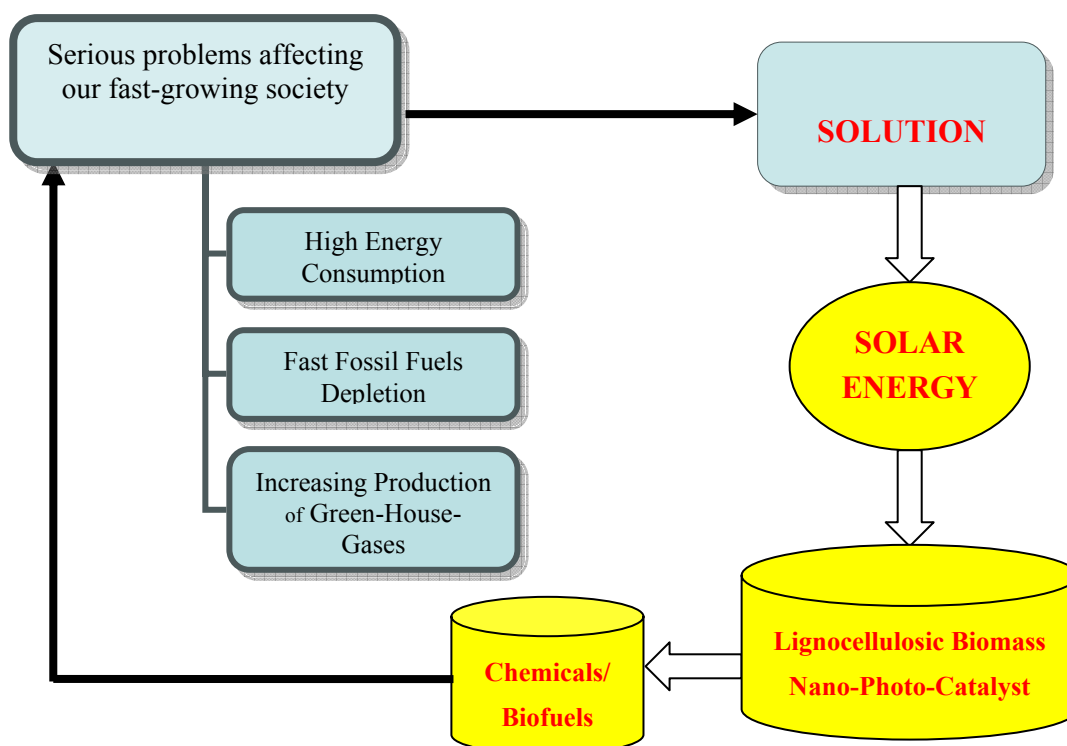
design routes for nanostructured photocatalytic solid materials in view of their applications in the selective transformation of lignocellulosic biomass to high value-added chemicals.

Keywords: heterogeneous photocatalysis; nanoparticles; biomass transformation; solar energy; biofuels

1. Introduction

Nanotechnology has attracted a great deal of attention in the last few years as miniaturisation and nanomaterials are often foreseen to be the key for a sustainable future. In a broadest sense, nanochemistry makes use of the tools of synthetic and materials chemistry to generate nanomaterials with size, shape and surface properties that can be designed to evoke a specific function with the aim to be utilised in a particular application/end use. Nanotechnology allows us to manipulate the matter on a molecular scale (much less than 100 nanometers), helping us to obtain valuable information for the synthesis of new materials with specific properties and with a high degree of reproducibility. In this regard, an important part of the scientific community is currently focused on a very challenging and relevant research's direction, which is the synthesis of novel nanostructured materials capable of absorbing the photonic energy coming from the sun with the aim of turning it into chemical or electrical energy (Scheme 1).

Scheme 1. The efficient use of solar energy and biomass is considered a potential solution for energy and environmental challenges.



Many of these nanostructured materials find important applications in heterogeneous photocatalysis [1–3] due to the relevance of this multidisciplinary area as well as the multipurpose character of the solutions derived from it. Photocatalysis offers the possibility of extending the spectrum of applications to a variety of processes, including oxidations and oxidative cleavages, reductions, isomerizations, substitutions, condensations and polymerizations.

Applying the concept of nanotechnology to heterogeneous catalysis helps us understand more accurately the transformations occurring on the catalyst's surface at a molecular level [4]. The synthesis of materials with nanometric dimensions will facilitate a better understanding of the reaction mechanisms as well as to design novel useful catalytic systems. Nevertheless, despite several advances in designing new methods to obtain reproducible materials, there still exist numerous difficulties which need to be overcome. From the point of view of the materials, photocatalysts require a series of characteristic properties depending on their applications, including particle size, specific surface area or space between the electronic levels, among others.

Research activities have more recently focused on advanced oxidation processes (AOPs) for the destruction of synthetic organic species resistant to conventional methods. AOPs rely on the *in-situ* generation of highly reactive radical species, mainly HO•, by using solar, chemical or other forms of energy [5,6]. The most attractive feature of AOPs is that this highly effective and strongly oxidizing radical facilitates the degradation of a wide range of organic chemical substrates with no selectivity.

Heterogeneous photocatalysis involves the acceleration of photoreactions in presence of a semiconductor catalyst. One of the most relevant applications of heterogeneous catalysis is photocatalytic oxidation (PCO) to the partial or total mineralisation of gas/liquid-phase contaminants to benign substances [7].

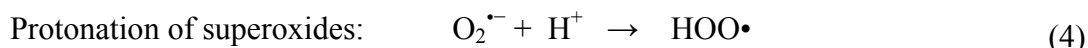
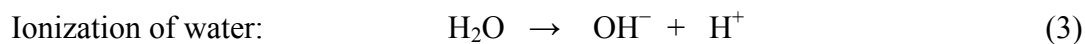
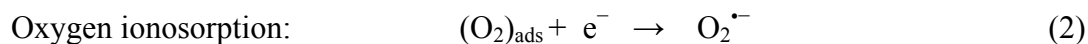
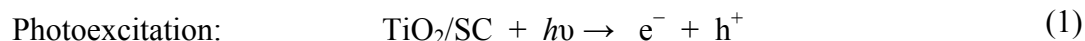
Titania photocatalysis, also referred to as the “Honda–Fujishima effect”, was first revealed by the pioneering research of Fujishima and Honda [8]. These authors disclosed the possibility of water-splitting by means of a photoelectrochemical cell comprising of an inert cathode and a rutile titania anode. The application of titania photocatalysis was subsequently extended to environmental applications. Frank and Bard [9] reported for the first time the application of TiO₂ in the photocatalytic oxidation of CN⁻ and SO₃²⁻ in aqueous medium under sunlight. Further reports on the photocatalytic reduction of CO₂ by Inoue *et al.* [10] attracted more interest in titania photocatalysis.

2. Basic Principles of Photocatalysis

Heterogeneous photocatalysis is a discipline which includes a large variety of reactions: organic synthesis, water splitting, photoreduction, hydrogen transfer, O₂¹⁸–O₂¹⁶ and deuterium–alkane isotopic exchange, metal deposition, disinfection and anti-cancer therapy, water detoxification, removal of gaseous pollutants, *etc.* [11,12]. Among them, titania-assisted heterogeneous photocatalytic oxidation has received more attention for many years as alternative method for purification of both air and water streams. The basic photophysical and photochemical principles underlying photocatalysis are already established and have been extensively reported [13,14].

A photocatalytic reaction is initiated when a photoexcited electron is promoted from the filled valence band of a semiconductor photocatalyst (SC) to the empty conduction band as the absorbed photon energy, $h\nu$, equals or exceeds the band gap of the semiconductor photocatalyst, leaving behind

a hole in the valence band. In concert, electron and hole pair ($e^- - h^+$) is generated. The following chain reactions have been widely accepted:



The hydroperoxyl radical formed in (4) has also scavenging properties similar to O_2 thus doubly prolonging the lifetime of photohole:



Both the oxidation and reduction can take place at the surface of the photoexcited semiconductor photocatalyst. Recombination between electron and hole occurs unless oxygen is available to scavenge the electrons to form superoxides ($\text{O}_2^{\bullet -}$), its protonated form the hydroperoxyl radical ($\text{HO}_2\bullet$) and subsequently H_2O_2 .

3. Mechanism of Titania-Assisted Photocatalysis

Titania has been widely used as a photocatalyst for generating charge carriers, thereby inducing reductive and oxidative processes, respectively [15]. Generally, ΔG is negative for titania-assisted aerobic photocatalytic reactions, as opposed to a photosynthetic reaction [11]. The corresponding acid A of the non-metal substituent is formed as by-product:



The [$>\text{Ti}^{\text{IV}}\text{OH}^{\bullet +}$] and [$>\text{Ti}^{\text{III}}\text{OH}$] represent the surface-trapped valence band electron and surface-trapped conduction band electrons, respectively. The surface-bound OH radical represented by [$>\text{Ti}^{\text{IV}}\text{OH}^{\bullet +}$] is chemically equivalent to the surface-trapped hole allowing the use of the former and latter terms interchangeably [16]. According to Lawless and Serpone [17], the trapped hole and a surface-bound OH radical are indistinguishable species. A good correlation occurs between charge carrier dynamics, their surface densities and the efficiency of the photocatalytic degradation over TiO_2 . In the last two decades, aqueous suspensions of TiO_2 have been probed by *pico*-second and more recently *femto*-second absorption spectroscopies [18,19]. Traditionally, an electron scavenger has been employed in such study. A *femto*-second spectroscopic study of $\text{TiO}_2/\text{SCN}^-$ aqueous system by Colombo and Bowman [18] indicated dramatic increase in the population of trapped charge carriers within the first few *pico*-seconds. The results also confirmed that for species adsorbed to TiO_2 , the hole-transfer reaction can successfully compete with the *pico*-second electron-hole recombination process. The following interfacial photochemical reactions were described (Figure 1):

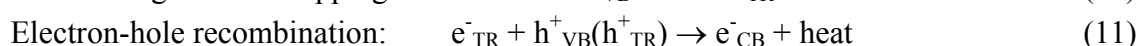
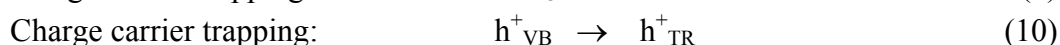
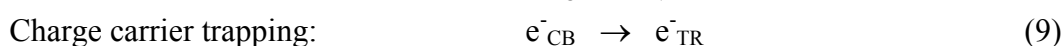
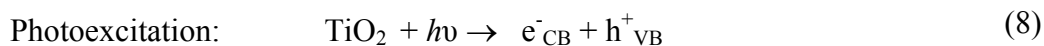
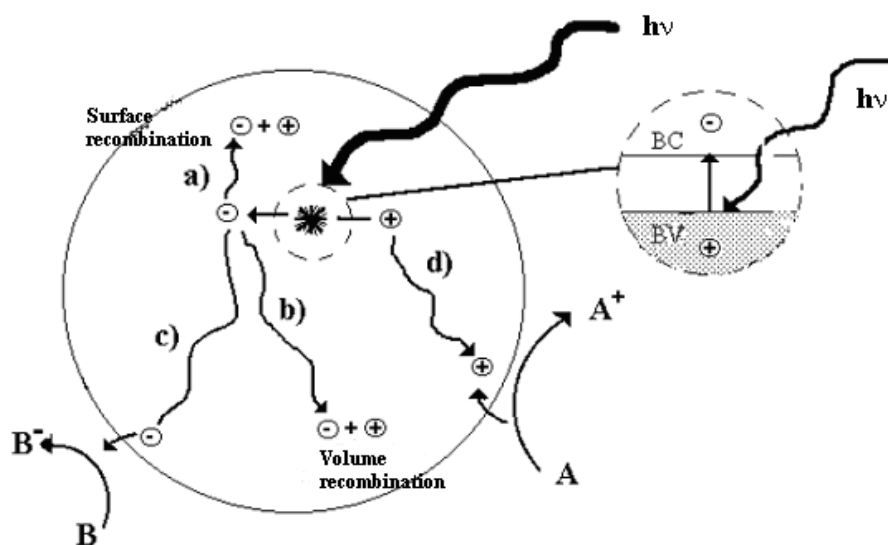


Figure 1. Photocatalytic process over TiO₂. Adapted from Programa Iberoamericano de Ciencia y Tecnología para el Desarrollo (*Red CYTED VIII-G*).



Photoholes have great potential to oxidize organic species directly (although mechanism not proven conclusively [7]) or indirectly via the combination with OH• predominant in aqueous solution [13,20]:



Mediation of radical oxidative species in photooxidation was evidenced by photo- and electro-luminescence spectra of TiO₂ electrodes in aqueous solutions measured as functions of the electrode potential and the solution pH [21]. It was found that the radical oxidative species originally absent accumulated after illumination under anodic bias. The primary photoreactions (1)–(11) indicate the critical role of charge carriers (electron–hole pair) in photooxidative degradation. Essentially, hydroxyl radicals (•OH), holes (h⁺), superoxide ions (O₂^{•−}) and hydroperoxyl radicals (•OOH) are highly reactive intermediates that will act concomitantly to oxidize large variety of organic pollutants including volatile organic compounds (VOCs) and bioaerosols [22,23]. It is however argued experimentally that the oxidative reaction on titania photocatalyst surface occurs mainly via the formation of holes (with quantum yield of 5.7×10^{-2}) not hydroxyl radicals formation (quantum yield 7×10^{-5}) [24]. As a photochemical application, TiO₂ photocatalysis is invariably affected by the surface properties of the TiO₂ particle. The photoinduced phenomenon is affected by quantum size. Anpo *et al.* [25] observed a blue shift and increase in reaction yield and photocatalytic activity as the diameter of the TiO₂ particles become smaller, especially below 10 nm. This observation was attributed to the suppression of radiationless transfer and the concurrent enhancement of the activities of the charge carriers.

4. Influence of Operational Parameters in Photocatalyst Efficiency

4.1. Light intensity

The photocatalytic reaction rate depends largely on the radiation absorption of the photocatalyst [26,27]. Recent reports revealed increase in the degradation rate with increase in light intensity during photocatalytic degradation [28,29]. The nature or form of the light does not affect the reaction pathway [30]. In other words, the band-gap sensitization mechanism does not have any significant influence in photocatalytic degradation. Unfortunately, only 5% of the total irradiated natural sunlight has sufficient energy to cause effective photosensitization [31]. Furthermore, energy losses due to light reflection, transmission and transformation into heat are inevitable in the photoprocess [32]. This limitation has greatly attracted more researchers to the applications of TiO₂ to decontamination/detoxification. The overall quanta of light absorbed by any photocatalyst or reactant is given by Φ_{overall} , the quantum yield:

$$\Phi_{\text{overall}} = \text{rate of reaction} / \text{rate of absorption of radiation}$$

where the rate of reaction (mol/time) accounts for moles of reactant/s consumed or product formed in the bulk phase and the rate of absorption of radiation (Einstein/time) relates to the amount (*i.e.*, mol or einstein) of photons at wavelength λ absorbed by the photocatalyst.

The light scattering in solid–liquid regimes is particularly significant. Quantum yield is thus experimentally difficult to determine as metal oxides in a heterogeneous regime including TiO₂ cannot absorb all the incident radiation due to refraction [33].

Another factor which limits photonic efficiency is the thermal recombination between electrons and holes [34]. For these reasons, it is argued that references to quantum yield or efficiency in heterogeneous system are not advised despite previous use of the term by previous references [35, 36]. A practical and simple alternative for comparing process efficiencies was suggested by defining the so-called *relative photonic efficiency* ζ_r [37]. A quantum yield can be subsequently determined from ζ_r , as:

$$\Phi = \zeta_r \Phi_{\text{compound}}$$

where Φ_{compound} is the quantum yield for the photocatalyzed oxidative disappearance of this chemical using a photocatalyst (e.g., Degussa P-25 TiO₂).

4.2. Nature and concentration of the substrate

Organic molecules which can effectively adsorb to the surface of the photocatalyst will be more susceptible to direct oxidation [38]. Thus, the photocatalytic degradation of aromatics depends on the substituent group. Nitrophenol has been reported to be a much stronger adsorbing substrate than phenol and therefore degrades faster [39]. In the degradation of chloroaromatics, Hugul *et al.* demonstrated that monochlorinated phenol degrades faster than di- or tri-chlorinated derivatives [40]. In general, molecules with electron-withdrawing groups including nitrobenzene and benzoic acid have been found to significantly adsorb in the dark compared to those with electron-donating groups [41].

The concentration of organic substrates in time is also dependent on photonic efficiency during photocatalytic oxidation [42]. At high-substrate concentrations, however, the photonic efficiency decreases and the titanium dioxide surface becomes saturated, thus leading to catalyst deactivation [43].

4.3. Nature of the photocatalyst

There is direct correlation between the surface of organic reagents and surface coverage of TiO₂ photocatalyst [44]. Kogo *et al.* reported that the number of photons hitting the photocatalyst actually controls the rate of the reaction [45]. The latter is an indication that the reaction takes place only in the adsorbed phase of the semiconductor particle. A very important parameter influencing the performance of nanomaterials in photocatalytic oxidation is the surface morphology, namely particle and agglomerate size [46]. Numerous forms of TiO₂ have been synthesized by different methods with the aim to achieve materials exhibiting desirable physical properties, activity and stability for photocatalytic application [47]. Evidently, there is a clear connection between the surface properties, the rational development of improved synthesis routes and the potential usefulness of the material prepared for particular applications [48,49]. For instance, smaller nano-particle sizes have been reported to give higher activities in gaseous phase photomineralisation of organic compounds employing nanostructured titanium dioxide [50].

4.4. Concentration of photocatalyst

The rate of photocatalytic reaction is strongly influenced by the photocatalyst concentration, as expected. Heterogeneous photocatalytic reactions are known to show proportional increase in photodegradation with increasing catalyst loadings [51]. Generally, in any given photocatalytic application, the optimum catalyst concentration must be determined, in order to avoid excess catalyst and ensure total absorption of efficient photons [52]. This is due to the observation of unfavourable light scattering and reduction of light penetration into the solution with an excess of photocatalyst [53].

4.5. pH

The pH of the solution is an important parameter in reactions taking place on particulate surfaces as it controls the surface charge properties of the photocatalyst and size of the formed aggregates [54]. In the current update of the points of zero charge (pzc, it describes the condition when the electrical charge density on a surface is zero) by Kosmulski, Degussa P-25 (80% anatase and 20% rutile) is reported to have pzc 6.9 [55]. The surface of titania can be protonated or deprotonated under acidic or alkaline conditions, respectively, according to the following reactions:



Thus, a titania surface will remain positively charged in acidic medium (pH < 6.9) and negatively charged in alkaline medium (pH > 6.9). Titanium dioxide is reported to have higher oxidizing activity at lower pH, but excess H⁺ at very low pH can decrease reaction rates [56].

The effect of pH on the photocatalytic reactions of organic compounds and adsorption on TiO₂ surfaces has been extensively studied [57,58]. Changes in pH can result in enhancement of the efficiency of photoremoval of organic pollutants in presence of titanium dioxide without affecting the rate equation [59]. Improved degradation of such compounds has been reported under optimized conditions [60].

4.6. Reaction temperature

Experimental studies on the dependence of the reaction rate with temperature in the degradation of organic compounds have been carried out since 1970s [61]. Many researchers established experimental evidences for the dependence of photocatalytic activity with temperature [62–66]. Generally, the increase in temperature enhances recombination of charge carriers and desorption process of adsorbed reactant species, resulting in a decrease of photocatalytic activity. These facts are in good agreement with the Arrhenius equation, for which the apparent first order rate constant $\text{Ln}k_{\text{app}}$ should increase linearly with $\exp(-1/T)$.

5. Properties and Characteristics of Photocatalysts: Titania vs Other Photocatalysts

An ideal photocatalyst for photocatalytic oxidation is characterized by the following attributes [11]:

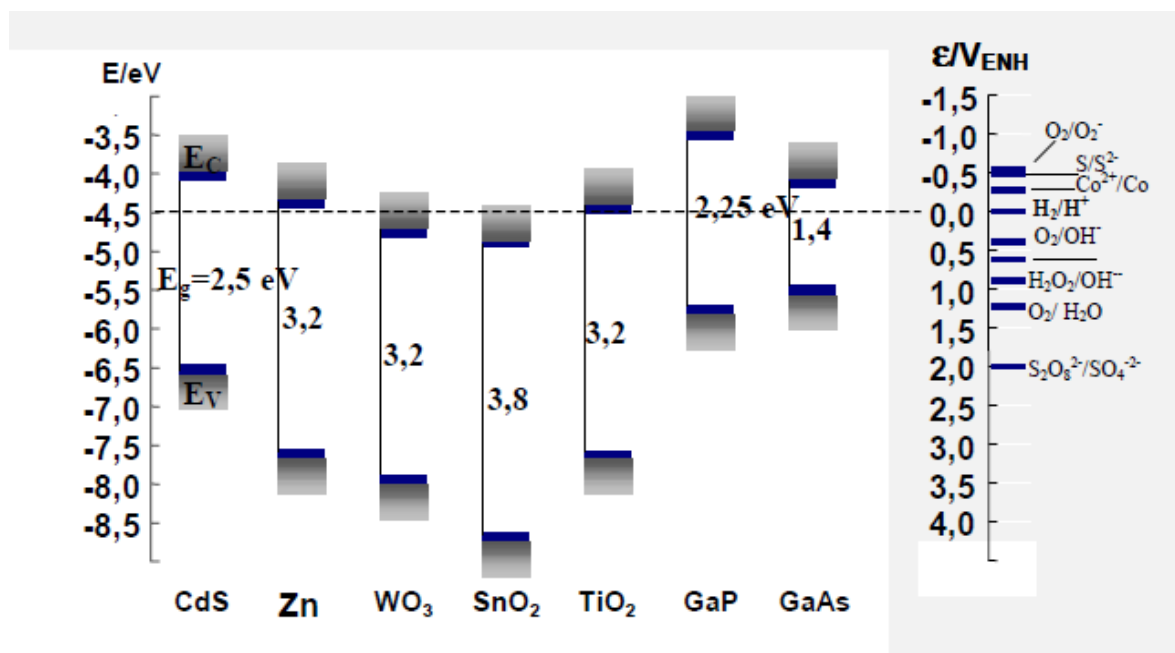
- (1) Photo-stability.
- (2) Chemically and biologically inert nature.
- (3) Availability and low cost.
- (4) Capability to adsorb reactants under efficient photonic activation ($h\nu \geq E_g$).

Titania is the most widely employed (nano)material in photocatalytic processes, although there are several (nano)materials currently considered as photocatalysts and/or supports for photocatalysis aside from titania. These include related metal oxides, metal chalcogenides, zeolites (as supports), *etc.*

5.1. Titania (TiO₂)

Nanometric size titania is by far the most widely employed system in photocatalysis due to its comparatively higher photocatalytic activity, low toxicity, chemical stability and very low cost. The anatase form of titania is reported to give the best combination of photoactivity and photostability [7]. Nearly all studies have focused on the crystalline forms of titania, namely anatase and rutile. The minimum band gap energy required for photon to cause photogeneration of charge carriers over TiO₂ semiconductor (anatase form) is 3.2 eV corresponding to a wavelength of 388 nm [67]. Practically, TiO₂ photoactivation takes place in the range of 300–388 nm. The photoinduced transfer of electrons occurring with adsorbed species on semiconductor photocatalysts depends on the band-edge position of the semiconductor and the redox potentials of the adsorbates [20]. The schematic diagram of band positions for various semiconductors is shown in Figure 2.

Figure 2. Diagram of conduction and valence band for various semiconductors. Adapted from Programa Iberoamericano de Ciencia y Tecnología para el Desarrollo (*Red CYTED VIII-G*).



5.1.1. Types of TiO₂ catalysts

The most frequently used TiO₂ photocatalyst is the Degussa P25 material [68–71]. Its particle size is about 25 nm and its surface area is very small (50 m²/g). Reducing the particle size, up to a few nanometres, has the benefit of increasing the external surface area. These small particles tend to agglomerate by strong interparticle forces when the nanometric size region is reached. Further decrease of the particle size to a few nanometers reaches one point below which quantum size effects also start to operate and the band gap of the semiconductor increases, blue-shifting the light absorption.

Titania in the form of photocatalyst titania materials of 1D dimensionality such as nanotubes, nanofibers and nanowires have also attracted attention for their use in photocatalysis [72–75]. In particular titania nanotubes with 10–100 nm in diameter and micrometric length have been the subject of intensive investigations. Compared to spherical particles, one-dimensional TiO₂ nanostructures could provide a high surface area and a high interfacial charge transfer rate. The carriers are free to move throughout the length of these nanostructures, which is expected to reduce the e⁻/h⁺ recombination probability. Titania nanotubes have a relatively high surface area compared to non-porous titania and time-resolved diffuse-reflectance spectroscopy has shown that charge recombination is disfavored by the tubular morphology of the titania. These titania nanotubes can be conveniently obtained starting from titania nanoparticles as, for instance P-25, that are digested under strong basic conditions in an autoclave at about 150 °C for several hours [76]. Annealing of these nanotube-TiO₂ at 400 °C for 3 h rendered nanotubes that are composed 100% by anatase. Laser flash photolysis of the nanotube-TiO₂ compared with conventional titania nanoparticles has allowed to estimate apparent

quantum yield of charge separation (Φ_{cs}). Table 1 lists some of the Φ_{cs} values measured for nanotube-TiO₂ compared with different conventional spherical nanoparticles powders.

Table 1. Surface area and photophysical data obtained by laser flash photolysis of nanotube-TiO₂ and other TiO₂ materials. Reproduced by permission of the Royal Society of Chemistry from reference 77.

TiO ₂ ^a	BET surface area/m ² g ⁻¹	Φ_{cs}	T _{1/2} /μs
nanotube-TiO ₂ -400	225	2.0	3.5 + 0.4
Standard TiO ₂ -1	300	7.1	0.6 + 0.2
Standard TiO ₂ -2	50	4.8	1.0 + 0.2
Standard TiO ₂ -3	10	1.6	0.7 + 0.2

^aTiO₂—commercial samples of spherical shaped nanoparticles.

Despite the research efforts in the search for novel photocatalysts over the last two decades, titania (in its anatase form) has remained a benchmark to compare with any emerging material candidate [78]. Zhang and Maggard also reported the preparation of hydrated form of amorphous titania with wider band energy gap than anatase and significant photocatalytic activity [79].

There are important drawbacks that severely limit the application of titanium dioxide photocatalyst as a general tool either to degrade organic pollutants in the gas or liquid phase or to perform useful transformations of organic compounds [80–87]. One of the most important limitations is the lack of TiO₂ photocatalytic activity with visible light [80,88,89]. The reason for this is that the anatase form of TiO₂ is a wide band gap semiconductor with a bandgap of 3.2 eV in most media, corresponding to an onset of the optical absorption band at about 350 nm. This onset of the TiO₂ absorption is also inadequate to achieve efficient solar light photocatalytic activity, since approx. 5% of the solar light energy can be absorbed by TiO₂. The above comments explain the continued interest in improving the photocatalytic efficiency of TiO₂.

5.1.2. Modified Titania systems for improved photocatalytic activity under visible light

Two general strategies have been developed to increase the photocatalytic activity of TiO₂ for visible light irradiation, namely the use of an organic dye as photosensitizer or doping TiO₂ with metallic and non-metallic elements [2,86,88,90–100].

The first route (using an organic dye that absorbs visible light) has worked very well under conditions where oxygen/air is excluded and the degradation of the dye is minimized by the efficient quenching of the dye oxidation state with an appropriate electrolyte [86,92–94,101–105]. Otherwise, particularly the dye becomes rapidly mineralized and the photocatalytic system loses its response towards visible light in the presence of oxygen. The mechanism of TiO₂ dye sensitization has been determined using time resolved subnanosecond laser flash photolysis techniques [101–104,106,107]. In dye sensitization, the most relevant points are the absorption spectrum of the dye in the visible region and the energy of the electron in the excited electronic state of the dye, which has to be high enough to be transferred to the semiconductor conduction band.

A second chemical route to promote titania photoresponse into the visible spectra is related to the doping of TiO₂ material either with metallic or non metallic elements [86,88,90–94]. In this case,

doping introduces occupied or unoccupied orbitals in the band gap region leading to negative or positive doping, respectively. A summary of some novel preparations of UV and visible light responsive titania photocatalysts developed over the last few years has been recently compiled [108].

Doping with metals

Pt doping of titania has recently attracted a great deal of attention due to promising improvement in photooxidation rate especially in gas phase. Pt–TiO₂ has been found to improve the photooxidation rate of ethanol, acetaldehyde and acetone in the gaseous phase [109,110]. A further development of mesoporous titania as photocatalyst has been reported by Li *et al.* [111]. These authors have prepared a photocatalyst constituted by mesoporous titania embedding gold nanoparticles (Au/TiO₂). Its preparation requires P-123 as structure directing agent, a mixture of TiCl₄ and Ti(OBu)₄ and AuCl₃ as the source of gold using ethanol as solvent. The gel is cast on a Petri dish to form a thin layer that is subsequently aged at 100°C to form a homogeneous mesostructured nanocomposite. Calcination at 350 °C in air removes the template while inducing crystallization of TiO₂ and formation of gold nanoparticles.

TiO₂ has also been doped with other metals, including V, Cr, Mn, Fe and Ni. The presence of the dopant was found to cause large shift in the absorption band of titanium dioxide towards the visible region. However, there are contradictory reports, particularly in the case of metal doping, describing either an increase or a decrease of the photocatalytic activity [2,12,97,112]. This controversy arises in part from the difficulty to establish valid comparisons between the photocatalytic activity of various solids testing different probe molecules and employing inconsistent parameters. Also, the doping procedure and the nature of the resulting material is very often not well defined and, most probably, controversial results can be obtained depending on the way in which the metal has been introduced. It also depends on the final concentration of the dopant. Thus, it has often been reported that there is an optimum doping level to achieve the maximum efficiency and beyond this point a decrease in photocatalytic activity is again observed [95,113]. Nevertheless, a generalised consensus has been reached with regards to the inappropriateness of metal doping as valid solution to enhance the photocatalytic activity of TiO₂.

Doping with non-metallic elements

Doping with carbon, nitrogen, sulfur and other non-metallic elements has been recently reported to introduce visible light absorption on titanium dioxide [88, 90,113–123]. Asahi *et al.* were the first to show an absorption increase in the visible region upon nitrogen doping [114]. This opened the way to study titania doping with non-metallic elements [98, 115,124]. However, due to corrosion and instability of doped materials, it remains to be seen whether non-metallic element doping can be regarded as a general and valid approach to increase the photocatalytic efficiency of titania.

The photophysical mechanism of doped TiO₂ is not yet understood but the p-type metal ion dopants (with valencies lower than that of Ti⁴⁺) are believed to act as acceptor centres as opposed to the p-type [80].

5.2. Binary metal oxides

In addition to TiO₂, there are some other traditional metal oxides, which have also been extensively investigated due to their specific advantages. Many metal oxide semiconductors, including ZnO, ZrO₂, Fe₂O₃ and WO₃, have been examined and used as photocatalysts for the degradation of organic contaminants [125]. Among them, ZnO, α -Fe₂O₃ and WO₃ are representative. However, they all have inherent drawbacks to be employed in photocatalysis. ZnO is easily photo-corroded under bandgap irradiation by photogenerated holes. WO₃ is a stable photocatalyst for O₂ evolution under visible light irradiation, but not suitable, for instance, for H₂ production due to its low conduction band level. α -Fe₂O₃ has the same problem as WO₃ and, moreover, is not very stable in acidic solutions.

A nanocrystalline mesoporous Ta₂O₅ photocatalyst for H₂ production was recently synthesized through a combined sol-gel process with a surfactant-assisted templating mechanism [126]. The effects of NiO as co-catalyst loading and doping with Fe have also been studied [126,127].

5.3. Metal sulfides

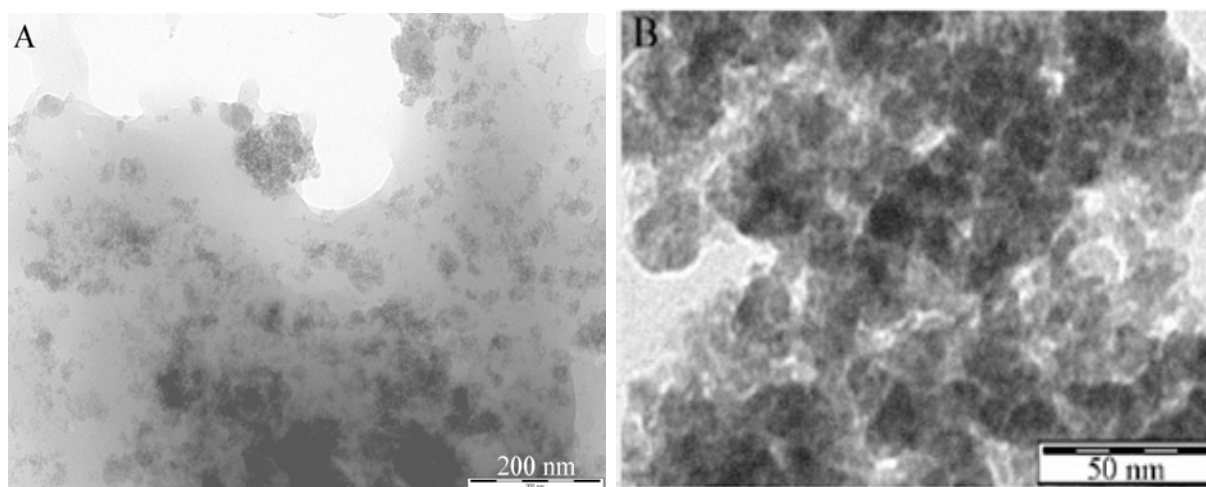
Metal sulfides are normally considered attractive candidates for visible light responsive photocatalysis. The valence band of metal sulfides normally consist of 3p orbitals of S, which result in a more occupied valence band and narrower bandgap as compared to metal oxides. Recent studies have focused on CdS, ZnS and their solid solutions.

CdS has a suitable bandgap (2.4 eV) and good band positions for visible light assisted water splitting. However, S²⁻ in CdS is easily oxidized by photogenerated holes, which is accompanied by the release of Cd²⁺ into solution, similar to ZnO. Such photo-corrosion is in fact a common problem to most metal sulfide photocatalysts.

Recent developments aiming at improving CdS and ZnS photocatalysts can be divided into four directions: (1) synthesis of one-dimensional and porous CdS; (2) doping and formation of solid solutions of CdS and ZnS; (3) addition of co-catalysts to CdS; and (4) development of support and matrix structures for CdS.

With regards to the synthesis of porous CdS, a solvothermal method was utilised to prepare CdS nanorods [128] and nanowires [129]. Mesoporous CdS nanoparticles with an average pore size of 5.4 nm and a particle size of 4–6 nm have also been prepared by template-free, ultrasonic-mediated precipitation at room temperature [130]. Bao *et al.* have also prepared nanoporous CdS, including nanosheets and hollow nanorods, by means of a two-step aqueous route, consisting of an initial precipitation of nanoporous Cd(OH)₂ intermediates and a subsequent S²⁻/OH⁻ ion exchange [131]. The obtained CdS nanostructures contain pores with 3 nm diameter. White *et al.* have also recently prepared CdS quantum dots supported on porous polysaccharides as novel contrast agents to provide better insights into the pore structure of materials that cannot be seen by simple microscopy imaging [132] (Figure 3).

Figure 3. Mesoporous polysaccharide supported CdS quantum dots. Adapted from reference [132].



Comparatively, ZnS possesses a bandgap too large to respond to visible light (3.6 eV). Doping and formation of solid solutions of ZnS and narrow bandgap semiconductors can enhance the visible light utilization of ZnS. ZnS and CdS have similar crystal structures, which make them form solid solutions easily.

$(\text{AgIn})_x\text{Zn}_{2(1-x)}\text{S}_2$ solid solutions between ZnS and AgInS_2 have a narrower bandgap. The absorption of the solid solutions shifted monotonically to longer wavelengths as the ratio of AgInS_2 to ZnS increased. Photophysical and photocatalytic properties of these nanomaterials were highly dependent on composition mainly due to a change in band position caused by the contribution of the Ag 4d and S 3p, and Zn 4s4p and In 5s5p orbitals to the valence and conduction bands, respectively [133].

6. Preparation of Photocatalysts

6.1. Sol-gel method: A promising route for TiO_2 nanophotocatalysts synthesis

The sol-gel process is currently considered one of the most promising alternatives due to its inherent advantages including low sintering temperature, versatility of processing and homogeneity at molecular level. This method allows the preparation of TiO_2 -anatase at low temperature. This phase has been extensively investigated because of its high activity in photocatalytic applications [84,134].

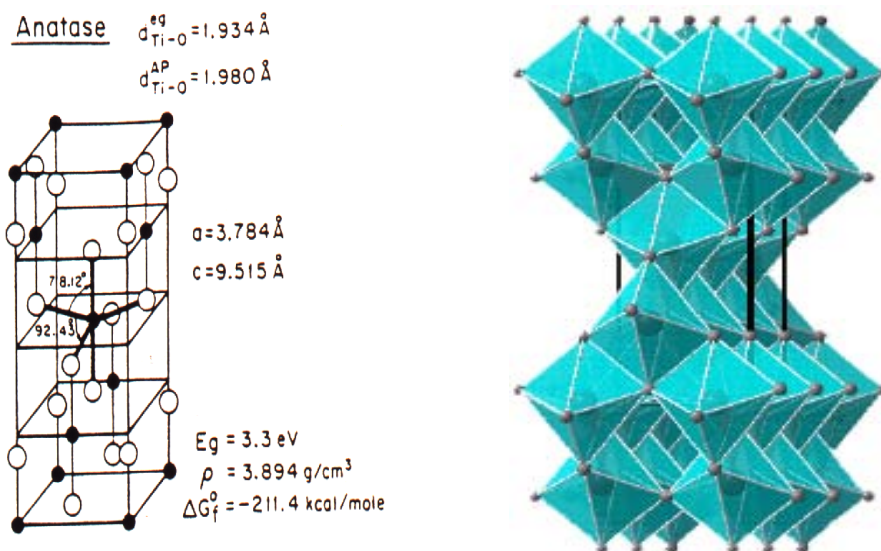
TiO_2 powders and gels with porous structure and high photocatalytic performance have been reported [135,136]. However, the preparation of porous TiO_2 films with high specific surface area is attracting more and more attention [137–139]. Photocatalytic processes are chemical reactions on the surface. The increase of surface area should improve the efficiency of the process as it implies larger contact surfaces exposed to the reagents [140,141]. Porous inorganic TiO_2 -anatase films can be obtained using templating membranes [142] or conventional alkoxide sol-gel route with the addition of surfactants [143]. Templates facilitate the retention of the initial polymer morphology up to the final porous structure. Polyethylene glycol is particularly suitable for modifying the porous structure of coatings [144,145] due to its complete decomposition at relatively low temperatures [146,147].

However, precise control on synthesis and deposition processes is crucial to achieve thick, crack-free and homogeneous coatings.

One of the advantages of sol-gel synthesis of mesoporous materials is the possibility to form uniform films on a substrate. Using the method studied in detail by Sanchez *et al.* [148,149] uniform films of mesoporous titania on glass can be obtained dipping the glass slide into an acidic solution of titanium alcoxide in ethanol. The surfactant concentration is lower than the critical micellar concentration (cmc) immediately after dipping the glass, but cmc is reached when the glass is gradually removed from solution (together with ethanol evaporation) and the surfactant starts to template the formation of thin layers of a mesoporous titanium oxide. The key point is to carefully control the rate of solvent evaporation to be sufficiently slow to allow the templation and oligomerization of the titanium oxide around the self assembled micelles created by the surfactant in its liquid crystal state.

Applying the above methodology, Stucky *et al.* prepared highly structured materials constituted by anatase nanoparticles (5–10 nm) ordered forming a mesoporous film of TiO₂ perpendicular to the glass slide [150]. The as-synthesized TiO₂ material is initially structured in the 5–100 nm length scale forming mesopores, but the walls are formed by an amorphous TiO₂ phase. Calcination of the material produces crystallization of the as-synthesized amorphous titanium dioxide into anatase phase (Figure 4) without destroying the mesoporous ordering of the film. Careful control of the calcination temperature (<500 °C) is also crucial to avoid the formation of the significantly less photocatalytic active rutile phase.

Figure 4. Structure of anatase.



6.2. Ultrasonic preparation of nanostructured photocatalysts

The use of non-conventional irradiation methods (e.g., sonication and microwave radiation) during the synthesis could be of help in order to avoid or at least reduce crystallite growth. In this sense, the use of ultrasonic irradiation during the synthetic procedure has been reported to facilitate the formation of smaller homogeneous nanoparticles and lead to an increase in surface area [2,151,152]

The presence of solid particles (metal supports) in the liquid system enhances the cavitation phenomenon under ultrasonic treatment [153,154] as the microbubbles tend to break up into smaller ones thus increasing the total number of regions of high temperature and pressure. Ultrasound can also enhance the mass transfer towards the liquid–solid interface [155].

Aging under sonication led to pure-anatase nanoparticles (the most active photocatalytic phase of titania) irrespective of the titanium precursor used and increased significantly the surface area of the nanostructured material. This enhancement in surface area resulted in an increase in molar conversion in the selective oxy-dehydrogenation of 2-propanol to acetone using Pt/TiO₂ as a photocatalyst [2].

In the same type of reaction, the subsequent photodeposition of platinum on Ti- and V-containing zeolites results in a sharp increase in molar conversion, low or negligible deactivation with time-on-stream and significant increase in selectivity to acetone (90–96%) [156].

6.3. Other non-conventional synthesis methodologies

Different methods have been used to prepare TiO₂ materials: reactive method [157], chemical vapour deposition, sputtering, pulsed laser deposition (PLD) [158] or hydrothermal method [159]. Mergel *et al.* [157] deposited films by electron beam evaporation of granular TiO₂ of purity 99.5% in a BAK640 high vacuum chamber pumped with a diffusion pump. The thickness of the films obtained by this method ranged from 0.9 to 2.4 mm.

Yamamoto *et al.* [158] synthesized TiO₂ films with anatase and rutile structure by pulsed laser deposition (PLD) with a NdYAG laser under controlled O₂ atmosphere. The same authors have also successfully prepared epitaxial anatase films on several types of oxide substrates with different lattice parameters (LaAlO₃, SrTiO₃, MgO and yttria-stabilized zirconia; YSZ). The high quality epitaxial rutile films were also grown on α -Al₂O₃ substrate. During deposition, substrates were maintained at 500 °C and exposed to 35 mtorr O₂ gas pressure. The typical thicknesses of epitaxial films were in the 200 to 880 nm range. From optical absorption measurements, the optical band gaps for anatase and rutile TiO₂ epitaxial films were evaluated to be 3.22 eV and 3.03 eV, respectively. The contribution of photoactivated electrons and holes to photocatalysis in these epitaxial TiO₂ films can be improved via further approaches to reduce crystal defects.

7. Photochemical Transformations of Biomass via Heterogeneous Photocatalysis

Photocatalysis is a good example of Green Chemistry. The relationship between Photocatalysis and Green Chemistry can be described in different ways. The name of the discipline itself is related to two of the so-called principles of Green Chemistry. “Photo” means light and if it is sunlight, as this is the case, there will be Energy Economy (6th Principle). On the other hand, catalytic processes are always preferable to non-catalytic ones (9th Principle). Furthermore, photocatalysis employed for the

transformation of biomass has impact on another two Green Chemistry principles, the use of renewable feedstocks (7th Principle) and the design for degradation (10th Principle).

Lignocellulosic substances (e.g., wood) undergo UV-induced degradative reactions. Early studies from Stillings and Van Nostrand on cellulose showed cotton fibers irradiated with UV-light under nitrogen atmosphere underwent photochemical transformations that led to an increase in the number of reducing sugars with a corresponding evolution of carbon monoxide and carbon dioxide [159].

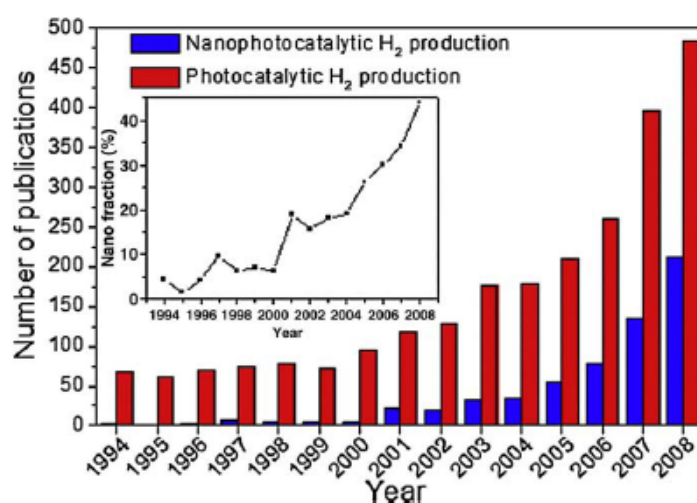
Desai and Shields also studied the photochemical degradation of cellulose filter paper 25 years later [160]. Working with rubber-stoppered static irradiation tubes that were initially filled with air (in contrast with the nitrogen-purged system of Stillings and Van Nostrand), they observed a spectrum of fully reduced and oxygenated hydrocarbons produced upon degradation. Such hydrocarbons were only observed after irradiation periods longer than 1–2 h, whereas no delay was observed in an initially oxygen-free atmosphere (*vide infra*). Biomass, the most versatile renewable resource, could therefore be turned into a wide range of chemicals and derivatives by means of photocatalysis.

In this section, we will highlight some of the most trendy and high potential processes for future development in the photochemical transformations of a range of biomass using heterogeneous photocatalysts.

7.1. Photocatalytic hydrogen production

Nanotechnology have boosted the modification of existing photocatalysts for the production of hydrogen and the discovery and development of new candidate materials, as shown in Figure 5. The rapidly increasing number of scientific publications on nanophotocatalytic H₂ production (1.5 times every year since 2004) provides clear evidences for the significance of this hot topic. Many papers studied the effect of different nanostructures and nanomaterials on the performance of photocatalysts, since their energy conversion efficiency is principally influenced by nanoscale properties.

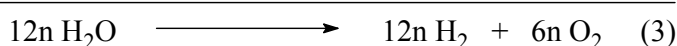
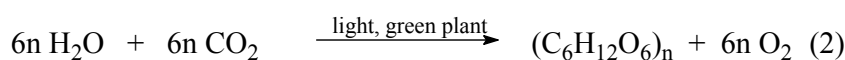
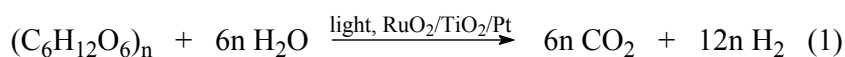
Figure 5. Evolution of the number of publications on (nano)photocatalytic production of hydrogen. Data from Web of Science (ISI, 2009).



Biomass sources have been utilized for the sustainable production of hydrogen [161,162]. A number of processes have been developed for this purpose (e.g., steam gasification [163], fast pyrolysis [162,164], and supercritical conversion [165,166]). However, these processes require harsh reaction conditions including high temperatures and/or pressures and consequently imply high costs.

Compared to these energy intensive thermochemical processes, photocatalytic reforming may be a good approach as this process can be driven by sunlight and performed at room temperature. Producing hydrogen by photocatalytic reforming of renewable biomass may also be more practical and viable than that of photocatalytic water-splitting due to its potentially higher efficiency. Water-splitting processes are relatively low efficient as limited by the recombination reaction between photogenerated electrons and holes [167].

However, to the best of our knowledge, there are only a few reports on the photocatalytic reforming of biomass to hydrogen in the literature. Pioneer studies were conducted in 1980 [168]. Kawai and Sakata reported that hydrogen could be generated from carbohydrates on RuO₂/TiO₂/Pt photocatalyst under 500W Xe lamp irradiation. The process is expressed as equation (1) together with the photosynthesis of carbohydrates by green plants (Equation 2), as follows:



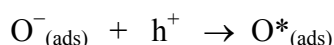
where (C₆H₁₂O₆)_n represents saccharose (n = 2), starch (n ≈ 100) or cellulose (n ≈ 1,000–5,000) after hydrolysis. This method may also be applied to decomposition of excrements containing cellulose, protein and fat, accompanied by the production of H₂ as biofuel.

The same authors subsequently reported that hydrogen could also be generated under identical conditions from other biomass sources including cellulose, dead insects, and waste materials [169–171]. These studies demonstrate the feasibility of the photocatalytic production of hydrogen from biomass.

Recent studies in H₂ production from the photocatalytic reforming of glucose (a model compound of cellulose) have also been performed using M/titania catalysts (where M is Pt, Rh, Ru, Au, or Ir; titania as commercial TiO₂ Degussa P25) [172]. Rh/TiO₂ was found to be the optimum catalytic system providing approx. 3500 μmol of H₂ for 0.5 g of catalyst and 5 h of irradiation.

Verykios *et al.* found that using alcohols (model compounds of biomass structure) as hole scavengers will result in increased quantum yields and enhanced rates of photocatalytic hydrogen production [173]. This is a good example of solar energy conversion into chemical energy (H₂ as an energy carrier). The reaction is a mild 100% selective oxidation process as well as a “chemical storage of light energy”.

Hydrogen can also be photocatalytically generated from chemicals or biomass using Pt/TiO₂ photocatalysts [174,175]. The high selectivity in this process was ascribed to the oxidation by a photoactive neutral, atomic oxygen species, detected by photoconductivity, and resulting from the neutralization of dissociatively chemisorbed O⁻(ads) species by positive photogenerated holes h⁺:



7.2. Photo-transformation (non-catalytic) of biomass: Solar gasification

Concentrated solar energy can supply the energy to drive the gasification process [176–179]. Solar gasification decreases the amount of biomass that needs to be burned in the gasification process, thus improving the process thermal efficiency.

Heat is provided to the gasification unit using concentrated solar gasifiers and specially designed solar reactors. Two different reactor configurations are used for solar gasification including direct irradiation of the reactants through a transparent window (usually made of fused quartz) and indirect heating through an opaque wall, in which the solar energy is absorbed by a nontransparent wall and transferred to inside particles. Solar energy is also used to dry wet biomass prior to the gasification process.

Figure 6. Concept of the reactor for solar gasification (Figure adapted from Adinberg *et al.* [179]. Reproduced from reference [77] by permission of the Royal Society of Chemistry.

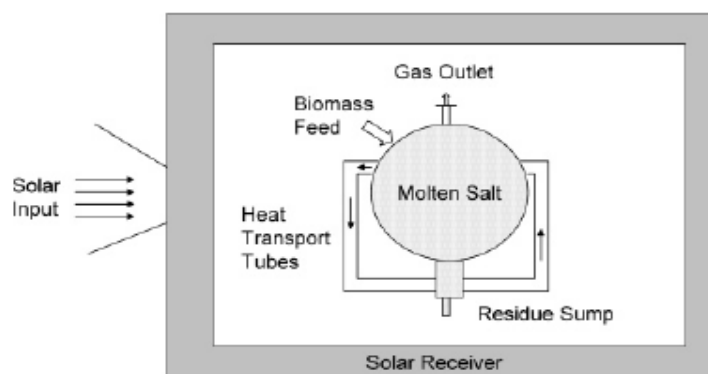


Figure 6 shows the concept of a solar gasification reactor based on a design by Adinberg *et al.* [179]. The reactor is a central spherically or cylindrically shaped reactor. An array of vertical tubes are evenly distributed around the reactor. Incoming solar radiation is absorbed in these tubes, which contain a molten salt. The tubes provide thermal storage of the solar energy as well as a reaction chamber. Secondary concentrating optics (compound parabolic concentrator) can be added to enhance the thermal concentration and reduce thermal losses. The absorbed radiation can heat the molten salt up to approximately 850 °C.

7.3. Other high added-value chemicals from photochemical conversion of biomass

The photoconversion of biomass into oxygenated hydrocarbons is another interesting alternative [180,181]. The oxygen sources for this reaction can be an aqueous media and/or alcohol/CH₃CN (more selective photo-oxidation) used to dissolve sensitizing ions (e.g., Fe³⁺, 2⁺), or “hydrated” carbohydrates.

Selective photo-oxidation of biomass can provide a wide range of high added-value chemicals including some of the so-called platform molecules (Table 2) [182]. Platform molecules are generally compounds with various functionalities that can be turned into a plethora of chemicals and products through different catalytic transformations including oxidations, hydrogenations, amidations and esterifications [183–185].

Table 2. Top twelve sugar-derived platform molecules [182].

Platform molecule	Structure
1,4-Diacids (succinic, fumaric and malic acids)	
2,5-Furandicarboxylic acid	
3-Hydroxypropionic acid	
Aspartic acid	
Glucaric acid	
Glutamic acid	
Itaconic acid	
Levulinic acid	
3-Hydroxybutyrolactone	
Glycerol	
Sorbitol	
Xylitol/Arabinitol	

8. Future Challenges and Prospects

The main drawback of heterogeneous photocatalysis (especially for degradation technology) is related to its inherently low quantum efficiency, only reaching 1% under optimised conditions (*i.e.*, only one out of one hundred incident photons is able to produce an oxidation/reduction step). Lamps can provide the necessary photons but the costs of photon production must be taken into account in the whole economics of the process and it can be very high. Sun can also give photons but only ca. 5% (ca. 30 Wm^{-2}) can be used by TiO_2 , and these values are realistically insufficient.

Three main challenges existing in heterogeneous photochemistry need therefore to be examined so as to understand what factors govern photochemical processes in heterogeneous systems.

Firstly, identification of the factors determining the activity of photocatalysts and subsequent realisation of how these factors influence their activity. Sometimes the aim is to achieve the greatest photocatalytic activity possible, whereas in others the desire may be to completely shut down the photochemical activity of the solids' surface.

Another major and no less significant challenge is to discover how to govern the selectivity of photocatalysts and what factors manipulate this selectivity. For example, even in conventional applications of photocatalysis in water and air purification, one may often wish to achieve complete mineralization of organic pollutants without necessarily producing hazardous by-products. Of greater importance for heterogeneous photocatalysis, however, may be the photochemical synthesis of desired high-value chemicals.

The last challenge deals with efforts on how to improve the spectral sensitivity of solid metal-oxide photocatalysts so that they can absorb considerable more light energy, thus significantly improving the efficiencies in processes.

Several future trends for further development are also currently under investigation. Most of such research lines are presently at their infancies but they are envisaged to hold a great potential in the near future. These include:

- the preparation of photocatalytic nanostructures capable of selective photocatalytic degradation of organic pollutants;
- novel preparation of ternary mixed oxide systems for photooxidative degradation;
- novel photocatalyst preparations from titanium oxo families as more members of the families become available in the future;
- designing of more reliable photocatalyst that can be photoactivated by visible and/or solar light;
- exploring the possibilities to work with other materials than titania (e.g., metal sulfides);
- photosensitizing TiO₂ in the visible by doping, especially by platinization and continue the investigation of anionic doping;
- taking advance of photocatalysis for preparative fine chemistry;
- use of photocatalysis as a new medical tool (e.g., in cancer treatment);
- novel photocatalysts for the production of energy: biohydrogen either from biomass or from photocatalytic splitting of water.

Acknowledgments

RL gratefully acknowledges Ministerio de Ciencia e Innovacion for the provision of a Ramón y Cajal Contract (RYC-2009–04199). J.C.C. (main author) would like to thank George Olah, G.K.S. Prakash and J.M. Marinas for their invaluable help in the area of energy and photocatalysis.

References and Notes

1. Serpone, N.; Emeline, A.V. Modelling heterogeneous photocatalysis by metal-oxide nanostructured semiconductor and insulator materials: factors that affect the activity and selectivity of photocatalysts. *Res. Chem. Intermed.* **2005**, *31*, 391–432.

2. Colmenares, J.C.; Aramendía, M.A.; Marinas, A.; Marinas, J.M.; Urbano, F.J. Synthesis, characterisation and photocatalytic activity of different metal doped titania systems. *Appl. Catal. A* **2006**, *306*, 120–127.
3. Wu, C.G.; Chao, C.C.; Kuo, F.T. Enhancement of the photocatalytic performance of TiO₂ catalysts via transition metal modification. *Catal. Today* **2004**, *97*, 103–112.
4. Somorjai, G.A.; Borodko, Y.G. Research in nanosciences-great opportunity for catalysis science. *Catal. Lett.* **2001**, *76*, 1–5.
5. Kudo, T.; Nakamura, Y.; Ruike, A. Development of rectangular column structured titanium oxide photocatalysts anchored on silica sheets by a wet process. *Res. Chem. Intermed.* **2003**, *29*, 631–639.
6. Bahnemann, D. Photocatalytic water treatment: solar energy applications. *Solar Energy* **2004**, *77*, 445–459.
7. Zeltner, W.A.; Tompkin, D.T. Shedding light on photocatalysis. *Ashrae Trans.* **2005**, *111*, 532–534.
8. Fujishima, A.; Honda, K. Electrochemical photolysis of water at a semiconductor electrode. *Nature* **1972**, *238*, 37–38.
9. Frank, S.N.; Bard, A.J. Heterogeneous photocatalytic oxidation of cyanide and sulfite in aqueous solutions at semiconductor powders. *J. Phys. Chem.* **1977**, *81*, 1484–1488.
10. Inoue, T.; Fujishima, A.; Konishi, S.; Honda, K. Photoelectrocatalytic reduction of carbon dioxide in aqueous suspensions of semiconductor powders. *Nature* **1979**, *277*, 637–638.
11. Carp, O.; Huisman, C.L.; Reller, A. Photoinduced reactivity of titanium dioxide. *Prog. Solid State Chem.* **2004**, *32*, 33–177.
12. Herrmann, J.M. Heterogeneous photocatalysis: fundamentals and applications to the removal of various types of aqueous pollutants. *Catal. Today* **1999**, *53*, 115–129.
13. Zhao, J.; Yang, X. Photocatalytic oxidation for indoor air purification: a literature review. *Build. Environ.* **2003**, *38*, 645–654.
14. Dung, N.T.; Khoa, N.V.; Herrmann, J.M. Photocatalytic degradation of reactive dye RED-3BA in aqueous TiO₂ suspension under UV-visible light. *Int. J. Photoenergy* **2005**, *7*, 11–15.
15. Kim, H.; Lee, S.; Han, Y.; Park, J. Preparation of dip-coated TiO₂ photocatalyst on ceramic foam pellets. *J. Mater. Sci.* **2005**, *40*, 5295–5298.
16. Horvath, I.T. *Encyclopedia of Catalysis*; John Wiley & Sons: New York, NY, USA, 2003.
17. Lawless, D.; Serpone, N.; Meisel, D. Role of hydroxyl radicals and trapped holes in photocatalysis. A pulse radiolysis study. *J. Phys. Chem.* **1991**, *95*, 5166–5170.
18. Colombo, D.P., Jr.; Bowman, R.M. Does interfacial charge transfer compete with charge carrier recombination? A femtosecond diffuse reflectance investigation of TiO₂ nanoparticles. *J. Phys. Chem.* **1996**, *100*, 18445–18449.
19. Yang, X.; Tamai, N. How fast is interfacial hole transfer? In situ monitoring of carrier dynamics in anatase TiO₂ nanoparticles by femtosecond laser spectroscopy. *Phys. Chem. Chem. Phys.* **2001**, *3*, 3393–3398.
20. Fujishima, A.; Rao, T.N.; Tryk, D.A. Titanium dioxide photocatalysis. *J. Photochem. Photobiol. C* **2000**, *1*, 1–21.

21. Nakato, Y.; Tsumura, A.; Tsubomura, H. Photo- and electroluminescence spectra from an n-titanium dioxide semiconductor electrode as related to the intermediates of the photooxidation reaction of water. *J. Phys. Chem.* **1983**, *87*, 2402–2405.
22. Jacoby, W.A.; Blake, D.M.; Fennell, J.A.; Boulter, J.E.; Vargo, L.A.M.; George, M.C.; Dolberg, Suzanne K. Heterogeneous photocatalysis for control of volatile organic compounds in indoor air. *Air Waste Management Assoc.* **1996**, *46*, 891–898.
23. Sleiman, M.; Conchon, P.; Ferronato, C.; Chovelon, J.M. Iodosulfuron degradation by TiO₂ photocatalysis: Kinetic and reactional pathway investigations. *Appl. Catal. B* **2007**, *71*, 279–290.
24. Ishibashi, K.; Fujishima, A.; Watanabe, T.; Hashimoto, K. Quantum yields of active oxidative species formed on TiO₂ photocatalyst. *J. Photochem. Photobiol. A* **2000**, *134*, 139–142.
25. Anpo, M.; Shima, T.; Kodama, S.; Kubokawa, Y. Photocatalytic hydrogenation of propyne with water on small-particle titania: Size quantization effects and reaction intermediates. *J. Phys. Chem.* **1987**, *91*, 4305–4310.
26. Curcó, D.; Giménez, J.; Addardak, A.; Cervera-March, S.; Esplugas, S. Effects of radiation absorption and catalyst concentration on the photocatalytic degradation of pollutants. *Catal. Today* **2002**, *76*, 177–188.
27. Ustinovich, E.A.; Shchukin, D.G.; Sviridov, D.V. Heterogeneous photocatalysis in titania-stabilized perfluorocarbon-in-water emulsions: Urea photosynthesis and chloroform photodegradation. *J. Photochem. Photobiol. A* **2005**, *175*, 249–252.
28. Qamar, M.; Muneer, M.; Bahnemann, D. Heterogeneous photocatalysed degradation of two selected pesticide derivatives, triclopyr and daminozid in aqueous suspensions of titanium dioxide. *J. Environ. Management* **2006**, *80*, 99–106.
29. Karunakaran, C.; Senthilvelan, S. Photooxidation of aniline on alumina with sunlight and artificial UV light. *Catal. Commun.* **2005**, *6*, 159–165.
30. Styliidi, M.; Kondarides, D.I.; Verykios, X.E. Visible light-induced photocatalytic degradation of Acid Orange 7 in aqueous TiO₂ suspensions. *Appl. Catal. B* **2004**, *47*, 189–201.
31. Wilke, K.; Breuer, H.D. The influence of transition metal doping on the physical and photocatalytic properties of titania. *J. Photochem. Photobiol. A* **1999**, *121*, 49–53.
32. Yang, L.; Liu, Z. Study on light intensity in the process of photocatalytic degradation of indoor gaseous formaldehyde for saving energy. *Energy Convers. Management* **2007**, *48*, 882–889.
33. Serpone, N.; Sauvé, G.; Koch, R.; Tahiri, H.; Pichat, P.; Piccinini, P.; Pelizzetti, E.; Hidaka, H. Standardization protocol of process efficiencies and activation parameters in heterogeneous photocatalysis: relative photonic efficiencies ζ_r . *J. Photochem. Photobiol. A* **1996**, *94*, 191–203.
34. Minero, C.; Vione, D. A quantitative evaluation of the photocatalytic performance of TiO₂ slurries. *Appl. Catal. B* **2006**, *67*, 257–269.
35. Aguado, M.A.; Anderson, M.A.; Hill Jr., C.G. Influence of light intensity and membrane properties on the photocatalytic degradation of formic acid over TiO₂ ceramic membranes. *J. Mol. Catal.* **1994**, *89*, 165–178.
36. Silva, C.G.; Wang, W.; Faria, J.L. Photocatalytic and photochemical degradation of mono-, di- and tri-azo dyes in aqueous solution under UV irradiation. *J. Photochem. Photobiol. A* **2006**, *181*, 314–324.

37. Serpone, N. Relative photonic efficiencies and quantum yields in heterogeneous photocatalysis. *J. Photochem. Photobiol. A* **1997**, *104*, 1–11.
38. Tariq, M.A.; Faisal, M.; Muneer, M.; Bahnemann, D. Photochemical reactions of a few selected pesticide derivatives and other priority organic pollutants in aqueous suspensions of titanium dioxide. *J. Mol. Catal. A* **2007**, *265*, 231–236.
39. Bhatkhande, D.S.; Kamble, S.P.; Sawant, S.B.; Pangarkar, V.G. Photocatalytic and photochemical degradation of nitrobenzene using artificial ultraviolet light. *Chem. Eng. J.* **2004**, *102*, 283–290.
40. Hugul, M.; Ercag, E.; Apak, R. Kinetic studies on UV-photodegradation of some chlorophenols using TiO₂ catalyst. *J. Environ. Sci. Health A* **2002**, *A37*, 365–283.
41. Palmisano, G.; Addamo, M.; Augugliaro, V.; Caronna, T.; Di Paola, A.; López, E.G.; Loddo, V.; Marci, G.; Palmisano, L.; Schiavello, M. Selectivity of hydroxyl radical in the partial oxidation of aromatic compounds in heterogeneous photocatalysis. *Catal. Today* **2007**, *122*, 118–127.
42. Friesen, D.A.; Morello, L.; Headley, J.V.; Langford, C.H. Factors influencing relative efficiency in photooxidations of organic molecules by Cs₃PW₁₂O₄₀ and TiO₂ colloidal photocatalysts. *J. Photochem. Photobiol. A* **2000**, *133*, 213–220.
43. Araña, J.; Martínez Nieto, J.L.; Herrera Melián, J.A.; Doña Rodríguez, J.M.; Gonzalez Diaz, O.; Pérez Peña, J.; Bergasa, O.; Alvarez, C.; Méndez, J. Photocatalytic degradation of formaldehyde containing wastewater from veterinarian laboratories. *Chemosphere* **2004**, *55*, 893–904.
44. Guillard, C.; Lachheb, H.; Houas, A.; Ksibi, M.; Elaloui, E.; Herrmann, J.M. Influence of chemical structure of dyes, of pH and of inorganic salts on their photocatalytic degradation by TiO₂ comparison of the efficiency of powder and supported TiO₂. *J. Photochem. Photobiol. A* **2003**, *158*, 27–36.
45. Kogo, K.; Yoneyama, H.; Tamura, H. Photocatalytic oxidation of cyanide on platinized titanium dioxide. *J. Phys. Chem.* **1980**, *84*, 1705–1710.
46. Ding, H.; Sun, H.; Shan, Y. Preparation and characterization of mesoporous SBA-15 supported dye-sensitized TiO₂ photocatalyst. *J. Photochem. Photobiol. A* **2004**, *169*, 101–107.
47. Gao, Y.; Liu, H. Preparation and catalytic property study of a novel kind of suspended photocatalyst of TiO₂-activated carbon immobilized on silicone rubber film. *Mater. Chem. Phys.* **2005**, *92*, 604–608.
48. Mohammadi, M.R.; Cordero-Cabrera, M.C.; Fray, D.J.; Ghorbani, M. Preparation of high surface area titania (TiO₂) films and powders using particulate sol-gel route aided by polymeric fugitive agents. *Sensors Actuators B* **2006**, *B120*, 86–95.
49. Diebold, U. The surface science of titanium dioxide. *Surf. Sci. Rep.* **2003**, *48*, 53–229.
50. Maira, A.J.; Yeung, K.L.; Soria, J.; Coronado, J.M.; Bolver, C.; Lee, C.Y.; Augugliaro, V. Gas-phase photo-oxidation of toluene using nanometer-size TiO₂ catalysts. *Appl. Catal. B* **2001**, *29*, 327–336.
51. Krysa, J.; Keppert, M.; Jirkovsky, J.; Stengl, V.; Subrt, J. The effect of thermal treatment on the properties of TiO₂ photocatalyst. *Mater. Chem. Phys.* **2004**, *86*, 333–339.
52. Saquib, M.; Muneer, M. TiO₂-mediated photocatalytic degradation of a triphenylmethane dye (gentian violet), in aqueous suspensions. *Dyes Pigments* **2003**, *56*, 37–49.

53. Chun, H.; Yizhong, W.; Hongxiao, T. Destruction of phenol aqueous solution by photocatalysis or direct photolysis. *Chemosphere* **2000**, *41*, 1205–1209.
54. Haque, M.M.; Muneer, M. Photodegradation of norfloxacin in aqueous suspensions of titanium dioxide. *J. Hazard. Mater.* **2007**, *145*, 51–57.
55. Kosmulski, M. pH-dependent surface charging and points of zero charge: III. Update. *J. Colloid Inter. Sci.* **2006**, *298*, 730–741.
56. Sun, J.; Wang, X.; Sun, J.; Sun, R.; Sun, S.; Qiao, L. Photocatalytic degradation and kinetics of Orange G using nano-sized Sn(IV)/TiO₂/AC photocatalyst. *J. Mol. Catal. A.* **2006**, *260*, 241–246.
57. Wang, W.Y.; Ku, Y. Effect of solution pH on the adsorption and photocatalytic reaction behaviors of dyes using TiO₂ and Nafion-coated TiO₂. *Colloid Surf. A Physicochem. Eng. Aspects* **2007**, *302*, 261–268.
58. Mrowetz, M.; Selli, E. Photocatalytic degradation of formic and benzoic acids and hydrogen peroxide evolution in TiO₂ and ZnO water suspensions *J. Photochem. Photobiol. A* **2006**, *180*, 15–22.
59. Shourong, Z.; Qingguo, H.; Jun, Z.; Bingkun, W. A study on dye photoremoval in TiO₂ suspension solution. *J. Photochem. Photobiol. A* **1997**, *108*, 235–238.
60. Mansilla, H.D.; Bravo, C.; Ferreyra, R.; Litter, M.I.; Jardim, W.F.; Lizama, C.; Freer, J.; Fernández, J. Photocatalytic EDTA degradation on suspended and immobilized TiO₂. *J. Photochem. Photobiol. A* **2006**, *181*, 188–194.
61. Kraeutler, B.; Bard, A.J. Heterogeneous photocatalytic decomposition of saturated carboxylic acids on titanium dioxide powder. Decarboxylative route to alkanes. *J. Am. Chem. Soc.* **1978**, *100*, 5985–5992.
62. Tunesi, S.; Anderson, M.A. Photocatalysis of 3,4-DCB in titanium dioxide aqueous suspensions; effects of temperature and light intensity; CIR-FTIR interfacial analysis. *Chemosphere* **1987**, *16*, 1447–1456.
63. Evgenidou, E.; Fytianos, K.; Poullos, I. Semiconductor-sensitized photodegradation of dichlorvos in water using TiO₂ and ZnO as catalysts. *Appl. Catal. B* **2005**, *59*, 81–89.
64. Muradov, N.Z.; Traissi, A.; Muzzey, D.; Painter, C.R.; Kemme, M.R. Selective destruction of airbourne VOCs. *Solar Energy* **1996**, *56*, 445–453.
65. Fu, X.; Clark, L.A.; Zeltner, W.A.; Anderson, M.A. Effects of reaction temperature and water vapor content on the heterogeneous photocatalytic oxidation of ethylene. *J. Photochem. Photobiol. A* **1996**, *97*, 181–186.
66. Soares, E.T.; Lansarin, M.A.; Moro, C.C. A study of process variables for the photocatalytic degradation of rhodamine B. *Brazilian J. Chem. Eng.* **2007**, *24*, 29–36.
67. Perkowski, J.; Bzdon, S.; Bulska, A.; Józwiak, W.K. Decomposition of detergents present in car-wash sewage by titania photo-assisted oxidation. *Polish J. Environ. Stud.* **2006**, *15*, 457–465.
68. Hoffmann, M.R.; Martin, S.T.; Choi, W.; Bahnemann, D.W. Environmental applications of semiconductor photocatalysis. *Chem. Rev.* **1995**, *95*, 69–96.
69. Hurum, D.C.; Gray, K.A.; Rajh, T.; Thurnauer, M.C. Recombination pathways in the degussa P25 formulation of TiO₂: surface versus lattice mechanisms. *J. Phys. Chem. B* **2005**, *109*, 977–980.

70. Hurum, D.C.; Agrios, A.G.; Gray, K.A.; Rajh, T.; Thurnauer, M.C. Explaining the Enhanced Photocatalytic Activity of Degussa P25 Mixed-Phase TiO₂ Using EPR. *J. Phys. Chem. B* **2003**, *107*, 4545–4549.
71. Ding, Z.; Lu, G.Q.; Greenfield, P.F. Role of the Crystallite Phase of TiO₂ in Heterogeneous Photocatalysis for Phenol Oxidation in Water. *J. Phys. Chem. B* **2000**, *104*, 4815–4820.
72. McCann, J.T.; Marquez, M.; Xia, Y. Melt coaxial electrospinning: a versatile method for the encapsulation of solid materials and fabrication of phase change nanofibers. *Nano Lett.* **2006**, *6*, 2868–2872.
73. Zhong, Z.; Ang, T.P.; Luo, J.; Gan, H.C.; Gedanken, A. Synthesis of one-dimensional and porous TiO₂ nanostructures by controlled hydrolysis of titanium alkoxide via coupling with an esterification reaction. *Chem. Mater.* **2005**, *17*, 6814–6818.
74. Xiong, C.; Balkus Jr., K.J. Fabrication of TiO₂ nanofibers from a mesoporous silica film. *Chem. Mater.* **2005**, *17*, 5136–5140.
75. Yuan, Z.Y.; Su, B.L. Titanium oxide nanotubes, nanofibers and nanowires. *Colloids Surf. A* **2004**, *241*, 173–183.
76. Tachikawa, T.; Fujitsuka, M.; Majima, T. Mechanistic insight into the TiO₂ photocatalytic reactions: design of new photocatalysts. *J. Phys. Chem. C* **2007**, *111*, 5259–5275.
77. Aprile, C.; Corma, A.; Garcia, H. Enhancement of the photocatalytic activity of TiO₂ through spatial structuring and particle size control: From subnanometric to submillimetric length scale. *Phys. Chem. Chem. Phys.* **2008**, *10*, 769–783.
78. Rajeshwar, K.; Chenthamarakshan, C.R.; Goeringer, S.; Djukic, M. Titania-based heterogeneous photocatalysis. Materials, mechanistic issues and implications for environmental remediation. *Pure Appl. Chem.* **2001**, *73*, 1849–1860.
79. Zhang, Z.; Maggard, P.A. Investigation of photocatalytically-active hydrated forms of amorphous titania, TiO₂.nH₂O. *J. Photochem. Photobiol. A* **2007**, *186*, 8–13.
80. Kitano, M.; Matsuoka, M.; Ueshima, M.; Anpo, M. Recent developments in titanium oxide-based photocatalysts. *Appl. Catal. A* **2007**, *325*, 1–14.
81. Thu, H.B.; Karkmaz, M.; Puzenat, E.; Guillard, C.; Herrmann, J.M. From the fundamentals of photocatalysis to its applications in environmental protection and in solar purification of water in arid countries. *Res. Chem. Intermed.* **2005**, *31*, 449–461.
82. Schiavello, M. *Heterogeneous Photocatalysis*; Kluwer Academic Publishers: Dordrecht, The Netherlands, 1997.
83. Legrini, O.; Oliveros, E.; Braun, A.M. Photochemical processes for water treatment. *Chem. Rev.* **1993**, *93*, 671–698.
84. Fox, M.A.; Dulay, M.T. Heterogeneous photocatalysis. *Chem. Rev.* **1993**, *93*, 341–357.
85. Ellis, D.F.; Al-Ekabi, H. *Photocatalytic Purification and Treatment of Water and Air*; Elsevier: Amsterdam, The Netherlands, 1993.
86. Pichat, P.; Guillard, C.; Maillard, C.; Amalric, L.; D'Oliveira, J.C. Titanium dioxide photocatalytic destruction of water aromatic pollutants: intermediates; properties-degradability correlation; effects of inorganic ions and titanium dioxide surface area; comparisons with hydrogen peroxide processes. *Trace Met. Environm.* **1993**, *3*, 207–223.

87. Cunningham, J.; Al-Sayyed, G.; Sedlak, P.; Caffrey, J. Aerobic and anaerobic TiO₂-photocatalysed purifications of waters containing organic pollutants. *Catal. Today* **1999**, *53*, 145–158.
88. Yamashita, H.; Takeuchi, M.; Anpo, M. Visible light sensitive photocatalysts. In *Encyclopedia of Nanoscience and Nanotechnology*; American Scientific Publishers: Stevenson Ranch, CA, USA, **2004**, 639-654.
89. Kisch, H.; Macyk, W. Visible light photocatalysis by modified titania. *ChemPhysChem* **2002**, *3*, 399–400.
90. Bacsa, R.; Kiwi, J.; Ohno, T.; Albers, P.; Nadtochenko, V. Preparation, testing and characterization of doped TiO₂ active in the peroxidation of biomolecules under visible light. *J. Phys. Chem. B* **2005**, *109*, 5994–6003.
91. Karakitsou, K.E.; Verykios, X.E. Effect of altermvalent cation doping of titania on its performance as a photocatalyst for water cleavage. *J. Phys. Chem.* **1993**, *97*, 1184–1189.
92. Jin, Z.; Zhang, X.; Li, Y.; Li, S.; Lu, G. 5.1% Apparent quantum efficiency for stable hydrogen generation over eosin-sensitized CuO/TiO₂ photocatalyst under visible light irradiation. *Catal. Commun.* **2007**, *8*, 1267–1273.
93. Jin, Z.; Zhang, X.; Lu, G.; Li, S. Improved quantum yield for photocatalytic hydrogen generation under visible light irradiation over eosin sensitized TiO₂—Investigation of different noble metal loading. *J. Mol. Catal. A* **2006**, *259*, 275–280.
94. Abe, R.; Sayama, K.; Arakawa, H. Dye-sensitized photocatalysts for efficient hydrogen production from aqueous I⁻ solution under visible light irradiation. *J. Photochem. Photobiol. A* **2004**, *166*, 115–122.
95. Chen, L.C.; Huang, C.M.; Tsai, F.R. Characterization and photocatalytic activity of K⁺-doped TiO₂ photocatalysts *J. Mol. Catal. A* **2007**, *265*, 133–140.
96. Fresno, F.; Guillard, C.; Coronado, J.M.; Chovelon, J.M.; Tudela, D.; Soria, J.; Herrmann, J.M. Photocatalytic degradation of a sulfonylurea herbicide over pure and tin-doped TiO₂ photocatalysts. *J. Photochem. Photobiol. A* **2005**, *173*, 13–20.
97. Ge, L.; Xu, M. Influences of the Pd doping on the visible light photocatalytic activities of InVO₄-TiO₂ thin films. *Mater. Sci. Eng. B* **2006**, *131*, 222–229.
98. Serpone, N. Is the band gap of pristine TiO₂ narrowed by anion- and cation-doping of titanium dioxide in second-generation photocatalysts? *J. Phys. Chem. B* **2006**, *110*, 24287–24293.
99. Rengaraj, S.; Li, X.Z. Enhanced photocatalytic activity of TiO₂ by doping with Ag for degradation of 2,4,6-trichlorophenol in aqueous suspension. *J. Mol. Catal. A* **2006**, *243*, 60–67.
100. Choi, W.; Termin, A.; Hoffmann, M.R. Effect of doped metal ions on the photocatalytic reactivity of TiO₂ quantum particles. *Angew. Chem. Int. Ed.* **1994**, *33*, 1091–1092.
101. Bauer, C.; Boschloo, G.; Mukhtar, E.; Hagfeldt, A. Interfacial electron-transfer dynamics in Ru(tcterpy)(NCS)₃-sensitized TiO₂ nanocrystalline solar cells. *J. Phys. Chem. B* **2002**, *106*, 12693–12704.
102. He, J.; Zhao, J.; Shen, T.; Hidaka, H.; Serpone, N. Photosensitization of Colloidal Titania Particles by Electron Injection from an Excited Organic Dye-Antennae Function. *J. Phys. Chem. B* **1997**, *101*, 9027–9034.

103. Kamat, P.V.; Das, S.; Thomas, K.G.; George, M.V. Ultrafast photochemical events associated with the photosensitization properties of a squaraine dye. *Chem. Phys. Lett.* **1991**, *178*, 75–79.
104. Kreller, D.I.; Kamat, P.V. Photochemistry sensitizing dyes: Spectroscopic and redox properties of cresyl violet. *J. Phys. Chem.* **1991**, *95*, 4406–4410.
105. Ohsaki, Y.; Masaki, N.; Kitamura, T.; Wada, Y.; Okamoto, T.; Sekino, T.; Niihara, K.; Yanagida, S. Dye-sensitized TiO₂ nanotube solar cells: Fabrication and electronic characterization. *Phys. Chem. Chem. Phys.* **2005**, *7*, 4157–4163.
106. Kroeze, J.E.; Savenije, T.J.; Warman, J.M. Electrodeless determination of the trap density, decay kinetics, and charge separation efficiency of dye-sensitized nanocrystalline TiO₂. *J. Am. Chem. Soc.* **2004**, *126*, 7608–7618.
107. Kay, A.; Humphry-Baker, R.; Graetzel, M. Artificial photosynthesis. 2. Investigations on the mechanism of photosensitization of nanocrystalline TiO₂ solar cells by chlorophyll derivatives. *J. Phys. Chem.* **1994**, *98*, 952–959.
108. Gaya, U.I.; Abdullah, A.H. Heterogeneous photocatalytic degradation of organic contaminants over titanium dioxide: A review of fundamentals, progress and problems. *J. Photochem. Photobiol. C* **2008**, *9*, 1–12.
109. Kryukova, G.N.; Zenkovets, G.A.; Shutilov, A.A.; Wilde, M.; Gunther, K.; Fassler, D.; Richter, K. Structural peculiarities of TiO₂ and Pt/TiO₂ catalysts for the photocatalytic oxidation of aqueous solution of Acid Orange 7 Dye upon ultraviolet light. *Appl. Catal. B* **2007**, *71*, 169–176.
110. Aramendia, M.A.; Colmenares, J.C.; Marinas, A.; Marinas, J.M.; Moreno, J.M.; Navio, J.A.; Urbano, F.J. Effect of the redox treatment of Pt/TiO₂ system on its photocatalytic behaviour in the gas phase selective photooxidation of propan-2-ol. *Catal. Today* **2007**, *128*, 235–244.
111. Li, H.; Bian, Z.; Zhu, J.; Huo, Y.; Li, H.; Lu, Y. Mesoporous Au/TiO₂ nanocomposites with enhanced photocatalytic activity. *J. Am. Chem. Soc.* **2007**, *129*, 4538–4539.
112. Lin, Y.J.; Tseng, S.L.; Huang, W.J.; Wu, W.J. Enhanced photocatalysis of pentachlorophenol by metal-modified titanium (IV) oxide. *J. Environ. Sci. Health, Part B* **2006**, *41*, 1143–1158.
113. Okato, T.; Sakano, T.; Obara, M. Suppression of photocatalytic efficiency in highly N-doped anatase films. *Phys. Rev. B: Condens. Matter Mater. Phys.* **2005**, *72*, 115124/1–115124/6.
114. Asahi, R.; Morikawa, T.; Ohwaki, T.; Aoki, K.; Taga, Y. Visible-light photocatalysis in nitrogen-doped titanium oxides. *Science* **2001**, *293*, 269–271.
115. Cong, Y.; Chen, F.; Zhang, J.; Anpo, M. Carbon and nitrogen-codoped TiO₂ with high visible light photocatalytic activity. *Chem. Lett.* **2006**, *35*, 800.
116. Di Valentin, C.; Pacchioni, G.; Selloni, A. Theory of carbon doping of titanium dioxide. *Chem. Mater.* **2005**, *17*, 6656–6665.
117. Li, D.; Haneda, H.; Labhsetwar, N.K.; Hishita, S.; Ohashi, N. Visible-light-driven photocatalysis on fluorine-doped TiO₂ powders by the creation of surface oxygen vacancies. *Chem. Phys. Lett.* **2005**, *401*, 579–584.
118. Ohno, T.; Tsubota, T.; Toyofuku, M.; Inaba, R. Photocatalytic activity of a TiO₂ photocatalyst doped with C⁴⁺ and S⁴⁺ ions having a rutile phase under visible light. *Catal. Lett.* **2004**, *98*, 255–258.
119. Sakthivel, S.; Janczarek, M.; Kisch, H. Visible light activity and photoelectrochemical properties of nitrogen-doped TiO₂. *J. Phys. Chem. B* **2004**, *108*, 19384–19387.

120. Tachikawa, T.; Tojo, S.; Kawai, K.; Endo, M.; Fujitsuka, M.; Ohno, T.; Nishijima, K.; Miyamoto, Z.; Majima, T. Photocatalytic oxidation reactivity of holes in the sulfur- and carbon-doped TiO₂ powders studied by time-resolved diffuse reflectance spectroscopy. *J. Phys. Chem. B* **2004**, *108*, 19299–19306.
121. Mrowetz, M.; Balcerski, W.; Colussi, A.J.; Hoffmann, M.R. Oxidative power of nitrogen-doped TiO₂ photocatalysts under visible illumination. *J. Phys. Chem. B* **2004**, *108*, 17269–17273.
122. Liu H.; Gao, L. (Sulfur, nitrogen)-codoped rutile-titanium dioxide as a visible-light-activated photocatalyst. *J. Am. Ceram. Soc.* **2004**, *87*, 1582–1584.
123. Sakthivel, S.; Kisch, H. Photocatalytic and photoelectrochemical properties of nitrogen-doped titanium dioxide. *ChemPhysChem* **2003**, *4*, 487–490.
124. Chu, S.Z.; Inoue, S.; Wada, K.; Li, D.; Suzuki, J. Fabrication and photocatalytic characterizations of ordered nanoporous X-doped (X = N, C, S, Ru, Te, and Si) TiO₂/Al₂O₃ films on ITO/glass. *Langmuir* **2005**, *21*, 8035–8041.
125. Konstantinou, I.K.; Sakkas, V.A.; Albanis, T.A. Photocatalytic degradation of propachlor in aqueous TiO₂ suspensions. Determination of the reaction pathway and identification of intermediate products by various analytical methods. *Water Res.* **2002**, *36*, 2733–2742.
126. Sreethawong, T.; Ngamsinlapasathian, S.; Suzuki, Y.; Yoshikawa, S. Nanocrystalline mesoporous Ta₂O₅-based photocatalysts prepared by surfactant-assisted templating sol-gel process for photocatalytic H₂ evolution. *J. Mol. Catal. A* **2005**, *235*, 1–11.
127. Jing, D.; Guo, L. Hydrogen production over Fe-doped tantalum oxide from an aqueous methanol solution under the light irradiation. *J. Phys. Chem. Solids* **2007**, *68*, 2363–2369.
128. Janet, C.M.; Viswanath, R.P. Large scale synthesis of CdS nanorods and its utilisation in photocatalytic H₂ production. *Nanotech* **2006**, *17*, 5271–5277.
129. Jang, J.S.; Joshi, U.A.; Lee, J.S. Solvothermal synthesis of CdS nanowires for photocatalytic hydrogen and electricity production. *J. Phys. Chem. C* **2007**, *111*, 13280–13287.
130. Sathish, A.; Viswanath, R.P. Photocatalytic generation of hydrogen over mesoporous CdS nanoparticle: Effect of particle size, noble metal and support. *Catal. Today* **2007**, *129*, 421–427.
131. Bao, N.Z.; Shen, L.M.; Takata, T.; Domen, K. Self-templated synthesis of nanoporous CdS nanostructures for highly efficient photocatalytic hydrogen production under visible light. *Chem. Mater.* **2008**, *20*, 110–117.
132. White, R.J.; Budarin, V.L.; Clark, J.H. Tuneable mesoporous materials from α -D-polysaccharides. *ChemSusChem*. **2008**, *1*, 408–411.
133. Tsuji, I.; Kato, H.; Kobayashi, H.; Kudo, A. Photocatalytic H₂ evolution reaction from aqueous solutions over band structure-controlled (AgIn)_xZn₂(1-x)S₂ solid solution photocatalysts with visible-light response and their surface nanostructures. *J. Am. Chem. Soc.* **2004**, *126*, 13406–13413.
134. Kato, K.; Tsuzuki, A.; Taoda, H.; Torii, Y.; Kato, T.; Butsugan, Y. Crystal structures of TiO₂ thin coatings prepared from the alkoxide solution via the dip-coating technique affecting the photocatalytic decomposition of aqueous acetic acid. *J. Mater. Sci.* **1994**, *29*, 5911–5915.
135. Imai, H.; Hirashima, H. Preparation of porous anatase coating from sol-gel-derived titanium dioxide and titanium dioxide-silica by water-vapor exposure. *J. Am. Ceram. Soc.* **1999**, *82*, 2301–2304.

136. Schattka, J.H.; Schukin, D.G.; Jia, J.; Antonietti, M.; Caruso, R.A. Photocatalytic activities of porous titania and titania/zirconia structures formed by using a polymer gel templating technique. *Chem. Mater.* **2002**, *14*, 5103–5108.
137. Cernigoj, U.; Stangar, U.L.; Trebse, P.; Krasovec, U.O.; Gross, S. Photocatalytically active TiO₂ thin films produced by surfactant-assisted sol–gel processing. *Thin Solid Film* **2006**, *495*, 327–332.
138. Bu, S.; Jin, Z.; Liu, X.; Yin, T.; Cheng, Z. Preparation of nanocrystalline TiO₂ porous films from terpineol-ethanol-PEG system. *J. Mater. Sci.* **2006**, *41*, 2067–2073.
139. Choi, H.; Stathatos, E.; Dionysiou, D.D. Sol-gel preparation of mesoporous photocatalytic TiO₂ films and TiO₂/Al₂O₃ composite membranes for environmental applications. *Appl. Catal. B.* **2006**, *63*, 60–67.
140. Yu, J.; Zhao, X.; Du, J.; Chen, W. Preparation, microstructure and photocatalytic activity of the porous TiO₂ anatase coating by sol-gel processing. *J. Sol–Gel Sci. Technol.* **2000**, *17*, 163–171.
141. Kotani, Y.; Matoda, T.; Marsuda, A.; Kogure, T.; Tatsumisago, M.; Minami, T. Anatase nanocrystal-dispersed thin films via sol-gel process with hot water treatment: Effects of poly(ethylene glycol) addition on photocatalytic activities of the films. *J. Mater. Chem.* **2001**, *11*, 2045–2048.
142. Schattka, J.H.; Wong, E.H.M.; Antonietti, M.; Caruso, R.A. Sol-gel templating of membranes to form thick, porous titania, titania/zirconia and titania/silica films. *J. Mater. Chem.* **2006**, *16*, 1414–1420.
143. Chen, Y.; Stathatos, E.; Dionysiou D.D. Microstructure characterization and photocatalytic activity of mesoporous TiO₂ films with ultrafine anatase nanocrystallite. *Surf. Coat. Technol.* **2008**, *202*, 1944–1950.
144. Bu, S.; Jin, Z.; Liu, X.; Du, H.; Cheng, Z. Preparation and formation mechanism of porous TiO₂ films using PEG and alcohol solvent as double-templates. *J. Sol-Gel Sci. Technol.* **2004**, *30*, 239–248.
145. Kajihara, K.; Yao, T. Macroporous morphology of the titania films prepared by a sol-gel dip-coating method from the system containing poly(ethylene glycol). IV. General principle of morphology formation and effect of heat treatment. *J. Sol-Gel Sci. Technol.* **2000**, *17*, 173–184.
146. Kajihara, K.; Nakanishi, K.; Tanaka, K.; Hirao, K.K.; Soga, N. Preparation of macroporous titania films by a sol-gel dip-coating method from the system containing poly(ethylene glycol). *J. Am. Ceram. Soc.* **1998**, *81*, 2670–2676.
147. Kajihara, K.; Yao, T. Macroporous morphology of the titania films prepared by a sol-gel dip-coating method from the system containing poly(ethylene glycol). II. Effect of solution composition. *J. Sol-Gel Sci. Technol.* **1998**, *12*, 193–201.
148. Crepaldi, E.L.; De Soler-Illia, G.J.A.A.; Grosso, D.; Cagnol, F.; Ribot, F.; Sanchez, C. Controlled formation of highly organized mesoporous titania thin films: from mesostructured hybrids to mesoporous nanoanatase TiO₂. *J. Am. Chem. Soc.* **2003**, *125*, 9770–9786.
149. Grosso, D.; de Soler-Illia, G.J.A.A.; Crepaldi, E.L.; Cagnol, F.; Sinturel, C.; Bourgeois, A.; Brunet-Bruneau, A.; Amenitsch, H.; Albouy, P.A.; Sanchez, C. Highly porous TiO₂ anatase optical thin films with cubic mesostructure stabilized at 700 °C. *Chem. Mater.* **2003**, *15*, 4562–4570.

150. Bartl, M.H.; Boettcher, S.W.; Frindell, K.L.; Stucky, G.D. 3-D Molecular assembly of function in titania-based composite material systems. *Acc. Chem. Res.* **2005**, *38*, 263–271.
151. Yu, J.C.; Yu, J.; Ho, W.; Zhang, L. Preparation of highly photocatalytic active nano-sized TiO₂ particles *via* ultrasonic irradiation. *Chem. Commun.* **2001**, 1942–1943.
152. Oh, C.W.; Seong, G.D.L.; Park, S.; Ju, C.S.; Hong, S.S. Synthesis of nanosized TiO₂ particles via ultrasonic irradiation and their photocatalytic activity. *React. Kinet. Catal. Lett.* **2005**, *85*, 261–268.
153. Suslick, K.S. Sonochemistry. *Science* **1990**, *247*, 1439–1445.
154. Jensen, J.N. Applications of ultrasound for the destruction of hazardous waste. *Hazard. Ind. Wastes* **1996**, *28*, 265–274.
155. Mason, T.J.; Luche, J.L. Ultrasounds as a new tool for synthetic chemists. In *Chemistry Under Extreme or Non-classical Conditions*; John Wiley & Sons: New York, NY, USA, 1997; pp. 317–380.
156. Aramendía, M.A.; Colmenares, J.C.; López-Fernández, S.; Marinas, A.; Marinas, J.M.; Urbano, F.J. Screening of different zeolite-based catalysts for gas-phase selective photooxidation of propan-2-ol. *Catal. Today* **2007**, *129*, 102–109.
157. Mergel, D.; Buschendorf, D.; Eggert, S.; Grammes, R.; Samser, B. Density and refractive index of TiO₂ films prepared by reactive evaporation. *Thin Solid Films* **2000**, *371*, 218–224.
158. Yamamoto, S.; Sumita, T.; Sugiharuto; Miyashita, A.; Naramoto, H. Preparation of epitaxial TiO₂ films by pulsed laser deposition technique. *Thin Solid Films* **2001**, *401*, 88–93.
159. Stillings, R.A.; Van Nostrand, R.J. The action of ultraviolet light upon cellulose. I. Irradiation effects. II. Postirradiation effects. *J. Am. Chem. Soc.* **1944**, *66*, 753–760.
160. Desai, R.L.; Shields, J.A. Photochemical degradation of cellulose material. *Makromol. Chem.* **1969**, *122*, 134–144.
161. Ni, M.; Leung, D.Y.C.; Leung, M.K.H.; Sumathy, K. An overview of hydrogen production from biomass. *Fuel Process Technol.* **2006**, *87*, 461–472.
162. Iwasaki, W. A consideration of the economic efficiency of hydrogen production from biomass. *Int. J. Hydrogen Energy* **2003**, *28*, 939–944.
163. Rapagna, S.; Jand, N.; Foscolo, P.U. Catalytic gasification of biomass to produce hydrogen rich gas. *Int. J. Hydrogen Energy* **1998**, *23*, 551–557.
164. Li, S.G.; Xu, S.P.; Liu, S.Q.; Yang, C.; Lu, Q.H. Fast pyrolysis of biomass in free-fall reactor for hydrogen-rich gas. *Fuel Process Technol.* **2004**, *85*, 1201–1211.
165. Watanabe, M.; Inomata, H.; Arai, K. Catalytic hydrogen generation from biomass (glucose and cellulose) with ZrO₂ in supercritical water. *Biomass Bioenergy* **2002**, *22*, 405–410.
166. Hao, X.H.; Guo, L.J.; Mao, X.; Zhang, X.M.; Chen, X.J. Hydrogen production from glucose used as a model compound of biomass gasified in supercritical water. *Int. J. Hydrogen Energy* **2003**, *28*, 55–64.
167. Ni, M.; Leung, M.K.H.; Leung, D.Y.C.; Sumathy, K. A review and recent developments in photocatalytic water-splitting using TiO₂ for hydrogen production. *Renewable Sust. Energy Rev.* **2006**, *11*, 401–425.
168. Kawai, T.; Sakata, T. Conversion of carbohydrate into hydrogen fuel by a photocatalytic process. *Nature* **1980**, *286*, 474–476.

169. Kawai, M.; Kawai, T.; Tamaru, K. Production of hydrogen and hydrocarbon from cellulose and water. *Chem. Lett.* **1981**, *8*, 1185–1188.
170. Kawai, T.; Sakata, T. Photocatalytic hydrogen production from water by the decomposition of poly(vinyl chloride), protein, algae, dead insects, and excrement. *Chem. Lett.* **1981**, *1*, 81–84.
171. Sakata, T.; Kawai, T. Hydrogen production from biomass and water by photocatalytic processes. *Nouv. J. Chem.* **1981**, *5*, 279–281.
172. Wu, G.P.; Chen, T.; Zhou, G.H.; Zong, X.; Li, C. H₂ production with low CO selectivity from photocatalytic reforming of glucose on metal/TiO₂ catalysts. *Sci. China B* **2008**, *51*, 97–100.
173. Patsoura, A.; Kondarides, D.I.; Verykios, X.E. Photocatalytic degradation of organic pollutants with simultaneous production of hydrogen. *Catal. Today* **2007**, *124*, 94–102.
174. Herrmann, J.M. From catalysis by metals to bifunctional photocatalysis. *Top. Catal.* **2006**, *39*, 3–10.
175. Pichat, P.; Herrmann, J.M.; Disdier, J.; Mozzanega, M.N.; Courbon, H. Photocatalytic hydrogen production from aliphatic alcohols over a bifunctional platinum on titanium dioxide catalyst. *Nouv. J. Chim.* **1981**, *5*, 627–636.
176. Rustamov, V.R.; Abdullayev, K.M.; Aliyev, F.G.; Kerimov, V.K. Hydrogen formation from biomass using solar energy. *Int. J. Hydr. Energy* **1998**, *23*, 649–652.
177. Reed, T. *Problems and Opportunities for Solar Energy in Biomass, Pyrolysis, and Gasification*. Report No. SERI/TP-332–495; Solar Energy Research Institute: Golden, CO, USA, 1979.
178. Antal, M.J.; Hofmann, L.; Moreira, J.R.; Brown, C.T.; Steenblik, R. Design and operation of a solar fired biomass flash pyrolysis reactor. *Solar Energy* **1983**, *30*, 299–312.
179. Adinberg, R.; Epstein, M.; Karni, J. Solar gasification of biomass: A molten salt pyrolysis study. *J. Solar Energy Eng.* **2004**, *126*, 850–857.
180. Timpa, J.D.; Griffin, G.W. Photoinduced electron transfer cleavage of lignocellulosics. *Cellulose Chem. Technol.* **1985**, *19*, 279–289.
181. Greenbaum, E.; Tevault, C.V.; Ma, C.Y. New Photosynthesis: direct photoconversion of biomass to molecular oxygen and volatile hydrocarbons. *Energy Fuels* **1995**, *9*, 163–167.
182. Werpy, T.; Pedersen, G. Top Value Chemicals from Biomass. Volume I-Results of Screening for Potential Candidates from Sugars and Synthesis Gas. U.S. Department of Energy report, August 2004.
183. Budarin, V.; Luque, R.; Macquarrie, D.J.; Clark, J.H. Towards a bio-based industry: benign catalytic esterifications of succinic acid in the presence of water. *Chem. Eur. J.* **2007**, *13*, 6914–6919.
184. Budarin, V.; Clark, J.H.; Luque, R.; Macquarrie, D.J.; Koutinas, A.; Webb, C. Tunable mesoporous materials optimised for aqueous phase esterifications. *Green Chem.* **2007**, *9*, 992–995.
185. Luque, R.; Clark, J.H.; Yoshida, K.; Gai, P.L. Efficient aqueous hydrogenation of biomass platform molecules using supported metal nanoparticles on Starbons®. *Chem. Commun.* **2009**, 5305–5307.